

**Weak-value amplification of the fast-light effect in rubidium vapor**

Mohammad Mirhosseini,<sup>1,\*</sup> Gerardo I. Viza,<sup>2</sup> Omar S. Magaña-Loaiza,<sup>1</sup> Mehul Malik,<sup>1,3</sup>  
John C. Howell,<sup>2</sup> and Robert W. Boyd<sup>1,4</sup>

<sup>1</sup>*Institute of Optics, University of Rochester, Rochester, New York 14627, USA*

<sup>2</sup>*Department of Physics, University of Rochester, Rochester, New York 14627, USA*

<sup>3</sup>*Institute for Quantum Optics and Quantum Information (IQOQI), Austrian Academy of Sciences, Boltzmanngasse 3, A-1090 Vienna, Austria*

<sup>4</sup>*Department of Physics, University of Ottawa, Ottawa, Ontario K1N 6N5, Canada*

(Received 3 February 2015; published 27 May 2016)

We use weak-value amplification to enhance the polarization-sensitive fast-light effect from induced Raman absorption in hot rubidium vapor. We experimentally demonstrate that projecting the output signal into an appropriate polarization state enables a pulse advancement of  $4.2 \mu\text{s}$ , which is more than 15 times larger than that naturally caused by dispersion. More significantly, we show that combining weak-value amplification with the dispersive response of an atomic system provides a clear advantage in terms of the maximum pulse advance achievable for a given value of loss. This technique has potential applications for designing novel quantum-information-processing gates and optical buffers for telecommunication systems.

DOI: [10.1103/PhysRevA.93.053836](https://doi.org/10.1103/PhysRevA.93.053836)

**I. INTRODUCTION**

Due to Kramers-Kronig relations, a sharp change in the absorption or transmission of an optical medium results in a large modification of the group index [1]. Controlling the group velocity using slow and fast light is an enabling technology with many applications in photonics [2–5]. Additionally, fast light provides a unique test bed for studying the fundamental physics behind superluminal pulse propagation. While slow light can be achieved with no appreciable loss using electromagnetically induced transparency (EIT) [6], one needs to operate close to the center of an absorption line to achieve a negative group index with a large magnitude [7]. However, the large amount of absorption often limits the applications of resonant effects, making it preferable to employ slow- or fast-light mechanisms based on off-resonant dispersion or resonant optical gain lines [8–10].

Here, we propose an alternative approach that is based on modifying a time advance by using weak values. A weak measurement is a generalized form of quantum measurements, in which a weak unitary interaction is followed by a strong projective measurement [11,12]. Unlike the standard measurements, the result of a weak measurement, known as a weak value, can be beyond the range of eigenvalues of the measured operator [13–15]. This property, known as weak-value amplification (WVA), has been used before to sensitively measure a variety of effects, such as a transverse beam deflection [16–19], phase [20], velocity [21], and time delay [22]. Further, it has been suggested that the weak-value amplification can be used to enhance nonlinear optical effects in the few-photon regime [23].

In this work, we amplify the negative time delay associated with the so-called superluminal pulse propagation of an optical pulse in hot rubidium vapor. The fast-light effect is caused by an induced Raman absorption profile of the rubidium hyperfine structure in a pump-probe nonlinear interaction. Due to the polarization sensitivity of this effect, the polarization

of an optical pulse is weakly coupled with its arrival time. By appropriately preparing and postselecting the polarization states of the pulse, we can effectively engineer the dispersion properties of the medium [22,24], and thus amplify the weak coupling between polarization and arrival time. Using this technique, we were able to advance the peak of an optical pulse by an amount that is up to 15 times larger than the original fast-light advancement.

The fast-light effect due to absorption and the enhancement due to weak-value amplification are both lossy processes. Here, we study how the achieved temporal advancement scales as a function of loss due to atomic absorption and compare it to the scaling as a function of loss due to postselection in WVA. Remarkably, we find that for a given value of loss, an optimized combination of both these processes provides a larger time advance than that obtained by just increasing the atomic absorption itself. In light of the ongoing debate on the usefulness of WVA [25–30], we find this result to be both timely and significant.

**II. TUNABLE GROUP DELAY FROM ATOMIC RESPONSE**

In a dispersive medium the group velocity and the phase velocity are not the same. The group velocity and the group index can be calculated from the standard results

$$v_g = c/n_g, \quad n_g = n + \omega \frac{dn}{d\omega}. \quad (1)$$

Slow and fast light correspond to the situations where  $n_g \gg 1$  and  $n_g < 1$ , respectively. Due to the Kramers-Kronig relations, a sharp change in the absorption coefficient can lead to a substantial change in the group index. A large pulse advance in fast light can be achieved by operating in a wavelength close to the center of an absorption line (see Fig. 1). However, the large amount of loss in this region limits the amount of maximum negative delay that can be achieved in practice.

We use a nonlinear process to induce a polarization-sensitive absorption line in an atomic vapor. Consider a three-level atomic  $\Lambda$  system, where levels 1 and 2 are connected via the signal field  $\frac{1}{2}\Omega_s e^{-i(\omega_s t - kz)} + \text{c.c.}$  and levels 2 and 3 are

\*mirhosse@optics.rochester.edu

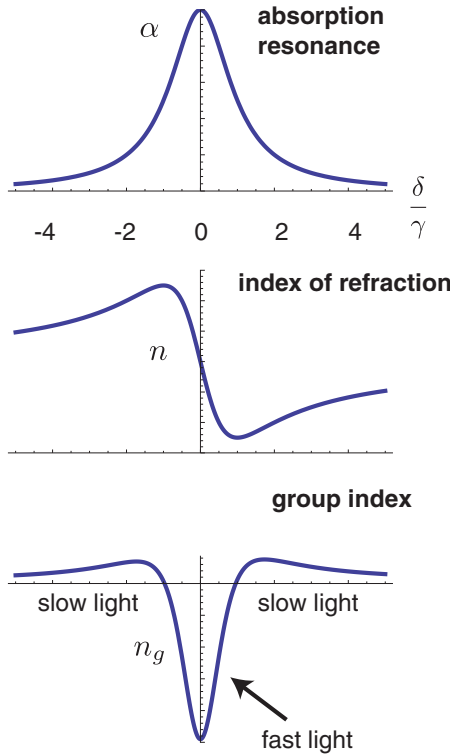


FIG. 1. Top panel: The absorption profile of a Lorentzian lineshape. Middle panel: The refractive index associated with the absorption line can be calculated using the Kramers-Kronig relations. Bottom panel: The group index for the same line. The horizontal axis for all the panels are identical and denote the frequency detuning from resonance, normalized by the line width of the Lorentzian line shape.

connected by a strong coupling field  $\frac{1}{2}\Omega_c e^{-i(\omega_c t - kz)} + \text{c.c.}$  The detunings are defined as  $\Delta_s = (\omega_2 - \omega_1) - \omega_s$ ,  $\Delta_c = (\omega_2 - \omega_3) - \omega_c$  and  $\delta = \Delta_s - \Delta_c$ . In this case the susceptibility at the signal frequency can be calculated as

$$\chi(\Delta, \delta, \Omega_c) = \beta \frac{\delta - i\gamma}{(\delta - i\gamma)(\Delta - i\Gamma/2) - |\Omega_c|^2/4}. \quad (2)$$

Here,  $\Gamma$  and  $\gamma$  are the excited-state spontaneous decay rate and the ground-state decoherence rates, respectively. The factor  $\beta$  is equal to  $N\mu^2/\hbar\epsilon_0$ , where  $N$  is the number density and  $\mu$  is the transition dipole moment between levels 1 and 2. This formula can explain many interesting results, including the electromagnetically induced absorption (EIA), that can be achieved for a large single-photon detuning.

For the case where  $\Delta \gg \Gamma$ , the expression for susceptibility can be approximated by a Lorentzian line shape

$$\chi(\Delta \gg \Gamma) = \beta \frac{|\Omega_c|^2}{4\Delta^2} \frac{\delta' + i\gamma'}{\delta'^2 + \gamma'^2}. \quad (3)$$

In the above  $\delta' = \delta - \delta_0$ ,  $\gamma' = \gamma + \gamma_0$ , where  $\delta_0 = |\Omega_c|^2 \Delta / (4\Delta^2 + \Gamma^2)$  and  $\gamma_0 = |\Omega_c|^2 \Gamma / (8\Delta^2 + 2\Gamma^2)$ .

The calculation above uses scalar fields to find the susceptibility and thus far we have neglected any dependence of the atomic response to the polarization of light. In a physical system, however, one needs to take into account

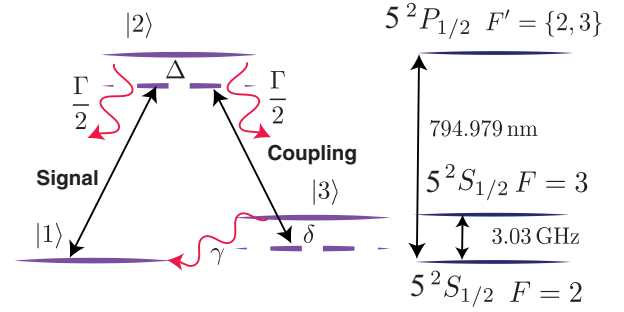


FIG. 2. Left panel: Schematic diagram of a three-level  $\Lambda$  system. Right panel: The hyperfine energy levels of  $^{85}\text{Rb}$ .

the vectorial nature of the electric fields in the coupling and the signal beams. For vector fields, the atomic selection rules set the energy levels that participate in the interaction, and the realization of the three-level system specified above may require a relation between the polarization states of coupling and signal beams. For the case of Rb atoms considered in this paper, we can realize the  $\Lambda$  system described above when the polarization of the signal beam is orthogonal to that of the coupling beam [31,32]. The energy diagram for the levels involved in our experiment are depicted in Fig. 2. In this configuration, the polarization component of the signal that is orthogonal to the polarization of the coupling beam experiences a narrow absorption line and consequently an advancement in pulse travel time with respect to propagation in vacuum. In contrast, the component of the signal polarized parallel to the coupling beam propagates through the medium with nearly no change in its group velocity.

When the signal field is composed of both polarization components, the differential time advance can be enhanced by performing a projective measurement in the polarization [22,24]. The modification of a time delay obtained in this manner is in fact an interference effect that can be fully understood using the classical theory of electromagnetism [33]. However, expressing this phenomenon within the weak-value formalism leads to a simpler and more elegant description that is easier to understand.

### III. WEAK-VALUE AMPLIFICATION OF THE TIME ADVANCE

We cast the propagation of an optical pulse through the atomic vapor in the language of quantum state measurement. The polarization and the temporal state of the signal beam before the cell can be described as

$$|\Psi_{\text{in}}\rangle = \frac{1}{\sqrt{T+1}}(|H\rangle + \sqrt{T}|V\rangle) \otimes |f(t)\rangle e^{-i\omega_0 t}, \quad (4)$$

where we have assumed a quasimonochromatic single optical mode with a pulse shape described by  $|f(t)\rangle$ . The horizontal and vertical polarization states are shown as  $|H\rangle$  and  $|V\rangle$  respectively. Since the polarization component  $|H\rangle$  attenuates upon propagation, it is initially weighted by a larger factor to precompensate for the effect of loss. The power transmission efficiency of propagation through the cell for a horizontally polarized signal beam is denoted by  $T$ . We now consider a case where the coupling beam is polarized in the vertical direction.

In this situation, the state of the signal beam in the output can be described as [6,34]

$$|\Psi_{\text{out}}\rangle = \sqrt{\frac{T}{T+1}} [ |H\rangle |f(t+t_0)\rangle + |V\rangle |f(t)\rangle ] e^{-i\omega_0 t}. \quad (5)$$

Here,  $t_0 = -(n_g - 1)\frac{L}{c}$  is the absolute value of the group delay for a propagation length  $L$ . We have dropped the common delay time between the two polarization states in order to simplify the notation. It is seen that horizontal polarization experiences attenuation and an advancement in time compared to the vertical component of the field. Additionally, we have assumed the optical path lengths in the medium for the two polarization components are equal. This results in the convenient phase difference of zero between the two polarization components in the output. In practice, a nonzero phase difference can always be pre-compensated by changing the polarization state of the input signal beam.

We use the weak value formalism for the case where the advancement time  $t_0$  is much smaller than the temporal duration of the pulse  $f(t)$ . Although our formalism closely follows that of Ref. [22], the large amount of time advance and the tunability provided by the atomic system in our experiment offers a degree of control absent from previous realizations. In the following section we provide a comparison of the loss vs time advance from WVA to the one obtained from the Kramers-Kronig relations. This analysis provides theoretical evidence for the efficacy of combining weak value amplification from the natural dispersive time advance from atomic response.

Assuming a Gaussian pulse shape, a postselection in the linear polarization state with an angle  $\theta$  with respect to the frame of the experiment results in

$$|\Psi_{PS}\rangle \approx \sqrt{\frac{T}{T+1}} (\cos\theta |H\rangle + \sin\theta |V\rangle) \otimes |f(t + A_w t_0)\rangle e^{-i\omega_0 t}. \quad (6)$$

Here,  $\Psi_{PS}$  is the polarization and the temporal state of the postselected beam.

The weak value  $A_w$  corresponds to the temporal shift of the optical pulse and can be calculated using the formula

$$A_w = \frac{\langle \Phi_\theta | \hat{A} | \Psi_{\text{in}} \rangle}{\langle \Phi_\theta | \Psi_{\text{in}} \rangle} = \frac{\cos\theta}{\sin\theta + \cos\theta}, \quad (7)$$

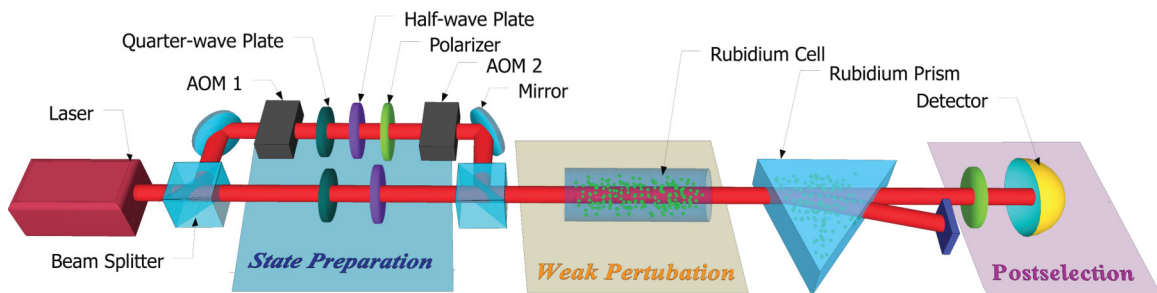


FIG. 3. Schematic of the experimental setup. The continuous wave laser beam is divided to two copies using a nonpolarizing beam splitter. The signal is frequency shifted using an acousto-optic modulator (AOM1) in double path (the figure shows a single path to simplify visualization). AOM2 is used to shape the signal beam to Gaussian pulses. The polarization state of the pump and the signal are controlled using wave plates. The postselection is done using a polarizer and a fast detector. The output photocurrent is analyzed by an oscilloscope.

where  $|\Phi_\theta\rangle$  is the postselected polarization state and the measurement operator is  $\hat{A} = |H\rangle\langle H|$ . It can be seen in Fig. 3 that choosing the postselection angle  $\theta$  close to  $45^\circ$  results in a large amplification factor  $A_w$ . More interestingly, it is possible to achieve a negative amplification and hence convert a time delay to a time advance and vice versa.

#### IV. EXPERIMENTAL IMPLEMENTATION

We realize the Raman absorption profile using warm atomic rubidium vapor. A sketch of the experimental setup is depicted in Fig. 3. The beam from a 795-nm narrow-line-width tunable diode laser is passed through a tapered-fiber amplifier to obtain a 10-mW coupling beam. The signal beam is obtained by frequency-shifting part of the laser beam by 3.035 GHz by double passing it through a tunable acousto-optic modulator. This separation corresponds to the ground-state hyperfine splitting of  $^{85}\text{Rb}$ . The power of the signal beam is set to  $100 \mu\text{W}$ .

The wavelength of the diode laser is tuned to have the signal beam detuned by 1.6 GHz to the blue of with the  $5^2S_{1/2} F = 3$  to  $5^2P_{1/2}$  transition. The coupling beam was therefore detuned to the blue of  $5^2S_{1/2} F = 2$  to  $5^2P_{1/2}$  transition. The coupling and the signal beams have Gaussian transverse profiles with  $1/e^2$  diameters of 3 and 1.8 mm, respectively. The coupling beam is prepared in the vertical polarization state and the signal beam is prepared in the diagonal polarization state. The two beams are then combined in a colinear fashion with a nonpolarizing beam splitter and are injected to an 8-cm rubidium cell.

The cell is heated using strip heaters inside a teflon tube enclosed by antireflection-coated windows at each end to achieve temperature stability. The cell is shielded from stray magnetic fields by a Mu-metal tubing. The vapor cell contains both rubidium isotopes in their natural abundance. In addition, we also have 20 Torr neon in the cell, which acts as a buffer gas. The temperature of the vapor cell is about  $80^\circ\text{C}$ , resulting in a number density of about  $10^{12} \text{cm}^{-3}$ . We use an atomic prism to filter out the coupling beam after the cell [35]. This prism contains isotopically pure  $^{87}\text{Rb}$  and is heated to  $100^\circ\text{C}$  to achieve a large dispersion ( $dn/d\lambda$ ). The coupling and the signal beams propagate at different angles once they exit the prism.

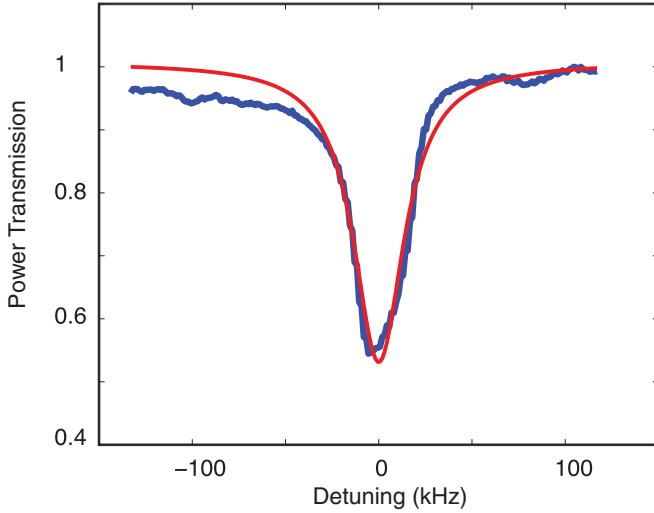


FIG. 4. Power transmission as a function of frequency detuning from Raman absorption. The blue curve presents the experimental data and the red curves shows the theoretical fit assuming a Lorentzian (with  $2\gamma = 34$  kHz) line shape for the susceptibility.

Figure 4 shows the measured power transmission of the signal beam as a function of detuning  $\delta'$ . This graph represents a typical result of the measurement of absorption. We have observed that the amount of absorption at the center of the dip varies, resulting in a transmission in the range  $T \approx 0.45$ – $0.55$  during the course of the experiment. We primarily attribute this change to fluctuations of the temperature of atomic prism. It can be seen that the measured transmission is in good agreement with a Lorentzian fit for the susceptibility. This observation verifies the assumption that the effect of Doppler broadening on susceptibility can be neglected for the case of copropagating coupling and signal beams [6,36].

We find the line width for the fitted Lorentzian profile in Fig. 4 to be  $2\gamma = 34$  kHz. The fitted susceptibility profile can be used to find the group index for operation at the center of the line width by using the Kramers-Kronig relations. We use Eq. (13) (derived in the next section) to find  $n_g = -7.5 \times 10^4$  for operation at the center of the absorption line. In our experiment, however, we use a nonzero two-photon detuning  $\delta$  to realize a small fractional delay for a Gaussian pulse. We use an acousto-optic modulator before the rubidium cell to carve Gaussian pulses with a FWHM width of  $20 \mu\text{s}$  from the signal beam. Upon propagation through the cell, the signal beam experiences the differential group delay caused by the copropagating coupling beam. We separate the signal beam from the coupling beam by using the atomic prism and then pass the signal beam through a polarizer. The output pulses from the polarizer are finally detected with a fast photodetector diode. We set the postselection state by setting the angle of the polarizer's axis. The top panel of Fig. 5 presents measured optical power as a function of time for four different postselection angles. We measure the time of arrival of the pulse by fitting a Gaussian wave form to the measured pulse and finding the position of its center. The comparison of the measured optical power for the horizontal and vertical polarizations give a value of  $t_0 = 0.28 \mu\text{s}$ , corresponding to a

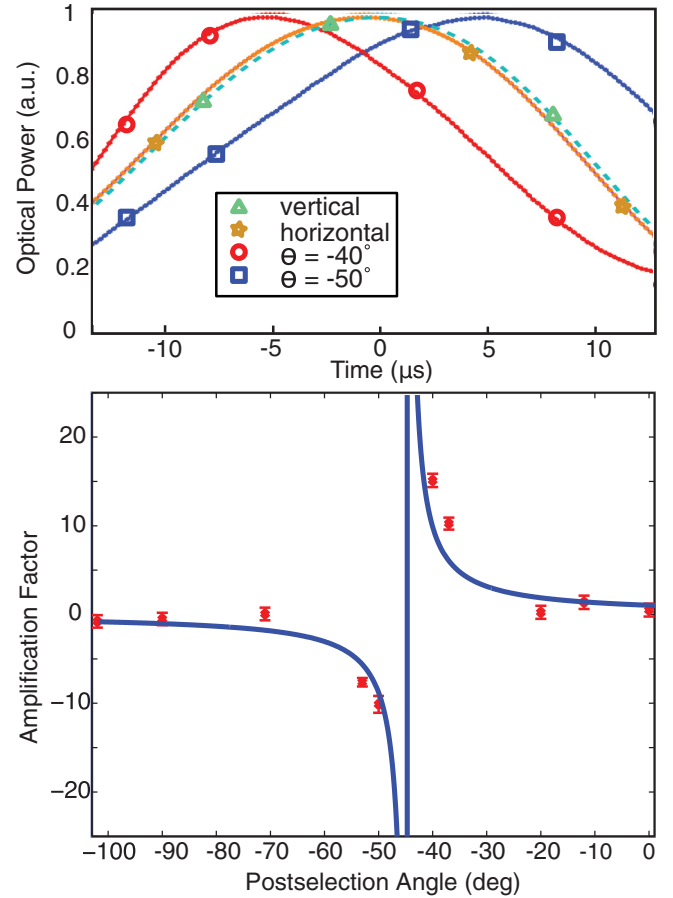


FIG. 5. Top: Measured optical power as a function of time for  $|H\rangle, |V\rangle$ , and for the output corresponding to the postselection angles  $\theta = -40^\circ$  and  $\theta = -50^\circ$ . The origin of time is set to the center of the pulse for the vertical polarization state. The markers are added to aid visualization and do not represent the data points. Bottom: The amplification factor as a function of postselection angle. The blue curve shows theory prediction from Eq. (7). The amplification factor is inferred from data by performing a Gaussian fit. The error bars correspond to the 95% confidence interval.

group index of  $n_g = -t_0 c/L \approx -1.0 \times 10^3$  and a fractional pulse delay of 1.4%.

The value of amplification factor as a function of postselection angle from the experiment is plotted in the bottom panel of Fig. 5. It can be seen that the delay gets drastically amplified as  $\theta$  approaches  $-45^\circ$ , and experiences a sign flip as it goes through it. The increase of loss in the proximity of  $\theta = -45^\circ$  eventually limits the maximum achievable amplification. The largest group delay measured in our experiment is equal to  $4.2 \mu\text{s}$ , which corresponds to an effective group index of  $n_g = -A_w t_0 c/L \approx -1.6 \times 10^4$  and a fractional pulse delay of 21%. It is evident that the experimental data points are in reasonable agreement with the theoretical prediction. We attribute the discrepancies between the theory line and the experimental results to the polarization instability of the signal beam after propagation through the rubidium cell. The instability is primarily caused by stray magnetic fields and temperature variations of the cell. Note that the theory curve is based on Eq. (7), which predicts a singularity for  $\theta = -45^\circ$ .

In practice, however, the maximum achievable amplification factor is limited as by the pulse width, and a more detailed analysis of the amplification factor has to take into account the effect of higher order terms in the weak-value expansion [37].

## V. THE SCALING OF GROUP DELAY WITH LOSS

The analysis and the experimental results above suggest that the WVA can be combined with the dispersive response of an atomic system to provide extra control over the value of group delay. However, to get an appreciable amplification factor one needs to postselect on a state that is nearly orthogonal to the input state. In this situation, the efficiency of the process is significantly reduced. This is, in fact, a universal property associated with weak values and the usefulness of WVA in the presence of this additional loss has been a topic of debate recently [25–30].

Before analyzing the effect of loss from postselection, we investigate the relation between loss and group delay from the atomic response. Using the susceptibility in Eq. (3) and assuming  $n \approx 1 + \frac{1}{2}\chi$  we get

$$n = \text{Re}[n] + i \text{Im}[n] = 1 + \beta \frac{|\Omega_c|^2}{8\Delta^2} \frac{\delta' + i\gamma'}{\delta'^2 + \gamma'^2}. \quad (8)$$

The group delay can be calculated using the real part of the group index. Assuming  $\Delta \gg \Gamma$ , and  $\Delta \gg |\Omega_c|$  we have

$$n_g|_{\delta'=0} = 1 + \beta \frac{|\Omega_c|^2}{8\Delta^2} \frac{\omega}{\gamma'^2}. \quad (9)$$

The group delay is related to the group index as  $\frac{Ln_g}{c}$ . The value of group delay includes the propagation time in vacuum. The differential time advance can be found as

$$t_0 = \beta \frac{L}{c} \frac{|\Omega_c|^2}{8\Delta^2} \frac{\omega}{\gamma'^2}. \quad (10)$$

We find the value of absorption at the center of the Lorentzian line as

$$\alpha = \frac{\omega}{c} \text{Im}[n] \Big|_{\delta'=0} = \frac{\beta}{8c} \frac{|\Omega_c|^2}{\Delta^2} \frac{\omega}{\gamma'}. \quad (11)$$

Subsequently, the power transmission efficiency is

$$T = \exp(-2\alpha L) = \exp(-2\gamma' t_0). \quad (12)$$

It is evident that increasing the absolute value of time advance via increasing the nonlinear interaction results in an exponential decrease in the transmission efficiency. Consequently, the group delay can be written as

$$t_{\text{atom}} = -\frac{\ln T}{2\gamma'}. \quad (13)$$

Equation (13) calculates the maximum amount of time advance that can be achieved from the atomic response for a given value of transmission efficiency.

The alternative strategy is to initially achieve a time advance  $\tilde{t}_0$  from the atomic response, at the cost of a reduction in the transmission efficiency for one of the polarization components to  $\tilde{T}$ . We then employ the WVA amplification to increase the amount of group delay at the cost of a further increase in the

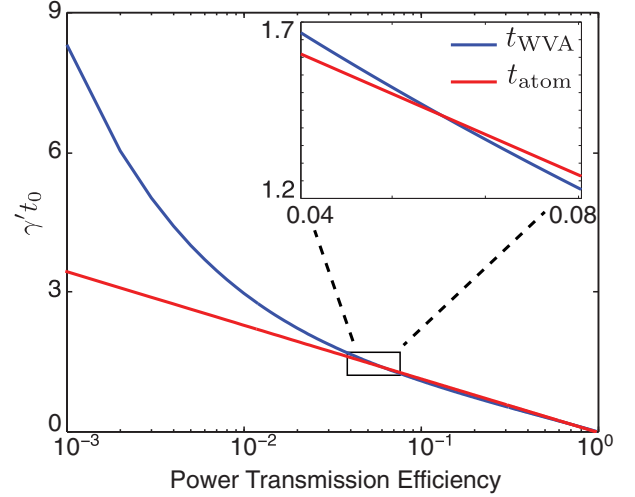


FIG. 6. Maximum achievable time advance as a function of transmission efficiency (calculated from theory).

loss. The input beam in this case is described by the state

$$|\Psi_{\text{in}}\rangle = \frac{1}{\sqrt{1+\tilde{T}}} (|H\rangle + \sqrt{\tilde{T}}|V\rangle) \otimes |f(t)\rangle e^{-i\omega_0 t}, \quad (14)$$

and the state after the postselection is equal to

$$|\Psi_{PS}\rangle = \sqrt{\frac{\tilde{T}}{1+\tilde{T}}} (\cos\theta|H\rangle + \sin\theta|V\rangle) \otimes |f(t + A_w \tilde{t}_0)\rangle e^{-i\omega_0 t}. \quad (15)$$

The total transmission efficiency for this strategy can be calculated by adding the postselection loss

$$T = |\langle \Psi_{PS} | \Psi_{PS} \rangle|^2 = \frac{2\tilde{T}}{1+\tilde{T}} \sin^2\left(\theta + \frac{\pi}{4}\right). \quad (16)$$

Similarly, the total time advance is equal to the contribution from the atomic response  $\tilde{t}_0$ , amplified by the postselection

$$t_0 = A_w \tilde{t}_0 = \frac{\cos\theta}{\sin\theta + \cos\theta} \tilde{t}_0. \quad (17)$$

We use the relation  $\tilde{t}_0 = -\frac{\ln \tilde{T}}{2\gamma'}$  for the atomic response to find the total time advance as

$$t_0(\theta) = \frac{1}{2\gamma'} \frac{\cos\theta}{\sin\theta + \cos\theta} \ln \left[ \frac{2\sin^2\left(\theta + \frac{\pi}{4}\right)}{T} - 1 \right]. \quad (18)$$

For a given value of loss, the maximum value of achievable time advance can be calculated by optimizing the absorption from the atomic response and the loss from postselection

$$t_{\text{WVA}} = \frac{1}{2\gamma'} \max_{\theta} \left( \frac{\cos\theta}{\sin\theta + \cos\theta} \ln \left[ \frac{2\sin^2\left(\theta + \frac{\pi}{4}\right)}{T} - 1 \right] \right). \quad (19)$$

The solutions of Eq. (19) are calculated numerically and plotted in Fig. 6, along with the solutions for Eq. (13). It is evident that the WVA procedure provides a slightly lower time advance for large values of transmission efficiency. However, as the transmission efficiency decreases, the time

advance obtained by using WVA grows rapidly, crossing the advancement obtained from the atomic response at  $T \approx 5\%$ . For all values of  $T$  lower than this value, WVA provides a larger time advance than that obtained from the atomic response alone. This showcases a clear instance where WVA provides an advantage for the estimation of a small interaction parameter.

## VI. CONCLUSIONS

We have used weak-value amplification to enhance the fast-light effect caused by electromagnetically induced absorption in warm rubidium vapor. By appropriately preparing and postselecting the polarization state of an optical pulse, we have obtained an advancement in time that is more than 15 times larger than that obtained from the atomic response. The enhancement from WVA can also be tuned to convert a time advance into a time delay and vice versa. Additionally, we have

shown that when the total transmission through the system is lower than 5%, the use of WVA provides a clear enhancement in the amount of time advance possible. Our technique provides an additional degree of freedom for controlling the group velocity of light, which may be useful for designing optical buffers and quantum-information-processing gates.

## ACKNOWLEDGMENTS

We gratefully acknowledge valuable discussions with S. Gillmer, J. Vornehm, Z. Shi, J. Ellis, and D. Gauthier. This work was supported by the DARPA/DSO InPho program, the Canadian Excellence Research Chair (CERC) program, and Army Research Office Grant No. W911NF-12-1-0263. O.S.M.L. acknowledges the support from CONACYT and the Mexican Secretaría de Educación Pública (SEP).

- 
- [1] R. W. Boyd, *Nonlinear Optics*, 3rd ed. (Academic Press, New York, 2003).
  - [2] R. M. Camacho, P. K. Vudiyasetu, and J. C. Howell, *Nat. Photon.* **3**, 103 (2009).
  - [3] K. F. Reim, J. Nunn, V. O. Lorenz, B. J. Sussman, K. C. Lee, N. K. Langford, D. Jaksch, and I. A. Walmsley, *Nat. Photon.* **4**, 218 (2010).
  - [4] Z. Shi, R. W. Boyd, R. M. Camacho, P. K. Vudiyasetu, and J. C. Howell, *Phys. Rev. Lett.* **99**, 240801 (2007).
  - [5] R. W. Boyd and D. J. Gauthier, in *Progress in Optics* (Elsevier, New York, 2002), p. 497.
  - [6] M. Fleischhauer, A. Imamoglu, and J. Marangos, *Rev. Mod. Phys.* **77**, 633 (2005).
  - [7] E. E. Mikhailov, V. A. Sautenkov, Y. V. Rostovtsev, and G. R. Welch, *JOSA B* **21**, 425 (2004).
  - [8] P. Siddons, N. C. Bell, Y. Cai, C. S. Adams, and I. G. Hughes, *Nat. Photon.* **3**, 225 (2009).
  - [9] J. Keaveney, I. G. Hughes, A. Sargsyan, D. Sarkisyan, and C. S. Adams, *Phys. Rev. Lett.* **109**, 233001 (2012).
  - [10] L. J. Wang, A. Kuzmich, and A. Dogariu, *Nature (London)* **406**, 277 (2000).
  - [11] Y. Aharonov, D. Z. Albert, and L. Vaidman, *Phys. Rev. Lett.* **60**, 1351 (1988).
  - [12] J. Dressel, M. Malik, F. M. Miatto, A. N. Jordan, and R. W. Boyd, *Rev. Mod. Phys.* **86**, 307 (2014).
  - [13] J. Dressel, S. Agarwal, and A. N. Jordan, *Phys. Rev. Lett.* **104**, 240401 (2010).
  - [14] J. Tollaksen, *J. Phys. A: Math. Theor.* **40**, 9033 (2007).
  - [15] A. Hosoya and Y. Shikano, *J. Phys. A: Math. Theor.* **43**, 385307 (2010).
  - [16] P. Dixon, D. Starling, A. Jordan, and J. Howell, *Phys. Rev. Lett.* **102**, 173601 (2009).
  - [17] N. W. M. Ritchie, J. G. Story, and R. G. Hulet, *Phys. Rev. Lett.* **66**, 1107 (1991).
  - [18] O. Hosten and P. Kwiat, *Science* **319**, 787 (2008).
  - [19] O. S. Magaña-Loaiza, M. Mirhosseini, B. Rodenburg, and R. W. Boyd, *Phys. Rev. Lett.* **112**, 200401 (2014).
  - [20] N. Brunner and C. Simon, *Phys. Rev. Lett.* **105**, 010405 (2010).
  - [21] G. I. Viza, J. Martinez-Rincon, G. A. Howland, H. Frostig, I. Shomroni, B. Dayan, and J. C. Howell, *Opt. Lett.* **38**, 2949 (2013).
  - [22] N. Brunner, V. Scarani, M. Wegmüller, M. Legré, and N. Gisin, *Phys. Rev. Lett.* **93**, 203902 (2004).
  - [23] A. Feizpour, X. Xing, and A. M. Steinberg, *Phys. Rev. Lett.* **107**, 133603 (2011).
  - [24] D. Solli, C. McCormick, R. Chiao, S. Popescu, and J. Hickmann, *Phys. Rev. Lett.* **92**, 043601 (2004).
  - [25] C. Ferrie and J. Combes, *Phys. Rev. Lett.* **112**, 040406 (2014).
  - [26] A. N. Jordan, J. Martinez-Rincon, and J. C. Howell, *Phys. Rev. X* **4**, 011031 (2014).
  - [27] G. C. Knee and E. M. Gauger, *Phys. Rev. X* **4**, 011032 (2014).
  - [28] G. I. Viza, J. Martinez-Rincon, G. B. Alves, A. N. Jordan, and J. C. Howell, *Phys. Rev. A* **92**, 032127 (2015).
  - [29] S. Pang and T. A. Brun, *Phys. Rev. Lett.* **115**, 120401 (2015).
  - [30] S. Pang, J. Dressel, and T. A. Brun, *Phys. Rev. Lett.* **113**, 030401 (2014).
  - [31] Y.-Q. Li and M. Xiao, *Phys. Rev. A* **51**, R2703 (1995).
  - [32] M. Xiao, Y.-Q. Li, S.-Z. Jin, and J. Gea-Banacloche, *Phys. Rev. Lett.* **74**, 666 (1995).
  - [33] B. Macke and B. Ségard, *Opt. Commun.* **281**, 12 (2008).
  - [34] P. K. Vudiyasetu, R. M. Camacho, and J. C. Howell, *Phys. Rev. A* **82**, 053807 (2010).
  - [35] D. J. Starling, S. M. Bloch, P. K. Vudiyasetu, J. S. Choi, B. Little, and J. C. Howell, *Phys. Rev. A* **86**, 023826 (2012).
  - [36] A. V. Tavčhenachev, V. I. Yudin, R. Wynands, M. Stähler, J. Kitching, and L. Hollberg, *Phys. Rev. A* **67**, 033810 (2003).
  - [37] K. Nakamura, A. Nishizawa, and M.-K. Fujimoto, *Phys. Rev. A* **85**, 012113 (2012).